

A computational study of the structure, lattice and defect properties of pure and doped F^- and OH^- -topaz

This article has been downloaded from IOPscience. Please scroll down to see the full text article.

2004 J. Phys.: Condens. Matter 16 S2771

(<http://iopscience.iop.org/0953-8984/16/27/012>)

View [the table of contents for this issue](#), or go to the [journal homepage](#) for more

Download details:

IP Address: 129.252.86.83

The article was downloaded on 27/05/2010 at 15:47

Please note that [terms and conditions apply](#).

A computational study of the structure, lattice and defect properties of pure and doped F⁻ and OH⁻-topaz

R A Jackson^{1,3} and M E G Valerio²

¹ Lennard-Jones Laboratories, School of Chemistry and Physics, Keele University, Keele, Staffs ST5 5BG, UK

² Departamento de Física, Universidade Federal de Sergipe, 49.100-000 São Cristovão, SE, Brazil

E-mail: r.a.jackson@chem.keele.ac.uk and mvalerio@fisica.ufs.br

Received 16 October 2003

Published 25 June 2004

Online at stacks.iop.org/JPhysCM/16/S2771

doi:10.1088/0953-8984/16/27/012

Abstract

This paper describes a computer modelling study of the F⁻ and OH⁻ forms of topaz, Al₂SiO₄(OH, F)₂. A potential model is developed, and used to calculate the perfect lattice and defect properties of both forms of the mineral. Excellent agreement between experimental and calculated phonon frequencies is obtained. Predictions are made of the probable intrinsic defect structure and of the location of dopant ions incorporated in ion implantation.

1. Introduction

Topaz is an aluminium fluoro-/hydroxy-silicate with fairly constant chemical composition Al₂SiO₄(OH, F)₂. The only major difference found between samples is the F/OH ratio. The structure consists of [SiO₄]⁴⁻ groups linking octahedral chains of Al[O₄(F, OH)₂] in a zigzag fashion parallel to the *c*-axis. Four of the six anions surrounding the Al³⁺ ion belong to [SiO₄]⁴⁻ tetrahedra; the remaining two are either F⁻ or OH⁻ groups. The structure is orthorhombic, with space group *Pbnm* [1]. Topaz has important potential applications in dosimeter devices, in which the F/OH ratio has been found to be of significance, particularly as it shows tissue equivalent dosimetry behaviour [2]. This paper describes a computational approach to the study of topaz. Computer modelling methods (see [3] for a recent mineralogical application) are applied using a combination of potentials transferred from previous aluminosilicate simulations [4], and newly obtained Al–O and Al–F potentials, fitted to the F⁻-topaz structure. Calculated perfect lattice properties for F⁻- and OH⁻-topaz are presented and compared with experimental values of infrared and Raman frequencies. Defect formation energies are reported for intrinsic defects in both materials, and conclusions drawn about the probable defect structure

³ Author to whom any correspondence should be addressed.

of both mineral forms. Finally, the location of metal dopants of interest in ion implantation studies is determined, the motivation being interest in how the dosimeter properties of topaz may be modified by ion implantation [5, 6].

2. Computer modelling

Computer modelling, based on lattice energy minimization, and the specification of interatomic interactions by effective potentials, can provide useful information on structures and properties of materials. The various stages involved in the study are summarized in this section. All calculations were performed using the GULP code [7].

2.1. The derivation of interatomic potentials

Where possible and appropriate, potentials from the literature were used. Aluminosilicate systems have been widely studied (see, for example, [4, 8]), which provide a starting point for the simulation of the silicate framework. Three-body bond-bending terms are used to describe the covalent nature of the silicon–oxygen bonds. The aluminium ions are octahedrally coordinated by oxygen or fluorine ions, and potentials to describe these interactions were fitted to the structure of F⁻-topaz. Oxygen and fluorine ions were described using the shell model to account for ionic polarizability. Potential parameters are given in table 1. For the interactions between the dopant ions and the lattice, potentials were fitted to the appropriate fluoride and oxide compounds, and are given in section (c) of table 1.

2.2. The calculation of structural and lattice properties

The technique of lattice energy minimization was used to calculate the structure and properties of F⁻- and OH⁻-topaz, noting that the F⁻-topaz structure was used to fit some of the potentials. The potential was then used to calculate phonon frequencies, for comparison with experimental results also reported.

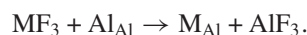
2.3. Point defects

Calculations of defect formation energies in both forms of topaz were carried out using the Mott–Littleton method [9, 10], which has been widely used in calculations of defect properties of inorganic materials; recent applications include a study of dopants in mixed metal fluorides [11] and the sillimanite–mullite system [3].

2.4. Calculations on doped topaz

Calculations have been carried out to obtain the substitution energies for Ti³⁺, Cr³⁺, Mn³⁺ and Fe³⁺ ions in F⁻- and OH⁻-topaz, along with solution energies, which give the total energy involved in the doping process, assuming a particular solution scheme.

- For substitution at the Al³⁺ site, no charge compensation is needed, and the solution energy is the overall energy of the process



- For solution at the Si⁴⁺ site, charge compensation by the formation of F⁻ or O²⁻ vacancies has been assumed, and the solution energy is the overall energy of one of the processes

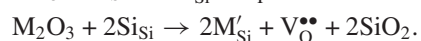


Table 1. Potentials used in the calculations.

Interaction	Potential	A (eV)	ρ (\AA)	C (eV \AA^6)
(a) Short range potentials for F ⁻ - and OH ⁻ -topaz				
Si _{core} -O _{shell}	Buckingham	1 283.90	0.320	10.66
Al _{core} -O _{shell}	Buckingham	1 460.30	0.299	0.0
F _{shell} -O _{shell}	Buckingham	464.540	0.3362	22.10
O _{shell} -O _{shell}	Buckingham	22 764.3	0.149	27.88
Si _{core} -F _{shell}	Buckingham	1 773.415	0.2571	0.0
Al _{core} -F _{shell}	Buckingham	1 773.415	0.2571	0.0
F _{shell} -F _{shell}	Buckingham	4 350.0	0.2753	15.83
Al _{core} -OH _{core}	Buckingham	1 142.678	0.2991	0.0
OH _{core} -OH _{core}	Buckingham	22 764.30	0.1490	27.88
H _{core} -OH _{core}	Buckingham	311.970	0.250	0.0
OH _{core} -O _{shell}	Buckingham	22 764.30	0.1490	0.0
OH _{core} -Si _{core}	Buckingham	983.557	0.3205	0.0
H _{core} -O _{shell}	Buckingham	1 400.0	0.250	0.0
(b) Other potential types				
O-Si-O	Harmonic	$k_b = 2.097 \text{ eV rad}^{-2}$	$\theta_0 = 109.47^\circ$	
H _{core} -OH _{core}	Morse	$D = 7.052 \text{ eV}$	$a = 2.198 \text{ \AA}^{-2}$	$r_0 = 0.948 \text{ \AA}$
F _{core} -F _{shell}	Harmonic	$Y = -1.378 e $	$k = 24.36 \text{ eV \AA}^{-2}$	
O _{core} -O _{shell}	Harmonic	$Y = -2.848 19 e $	$k = 74.92 \text{ eV \AA}^{-2}$	
(c) Potentials for dopant-lattice interactions				
M	A (M _{core} -F _{shell}) (eV)	ρ (M _{core} -F _{shell}) (\AA)	A (M _{core} -O _{shell}) (eV)	ρ (M _{core} -O _{shell}) (\AA)
Ti	3500.0	0.2570	1715.7	0.3069
Cr	2050.0	0.2295	6123.7	0.2295
Mn	2540.0	0.2570	1257.9	0.3214
Fe	2300.0	0.2295	1102.4	0.3299

The calculation of solution energies may be illustrated for the case of substitution at the Al³⁺ site:

$$E_{\text{sol}}(\text{Al}^{3+}) = -E_{\text{latt}}(\text{MF}_3) + E_{\text{subs}}(\text{Al}^{3+}) + E_{\text{latt}}(\text{AlF}_3).$$

In this expression, $E_{\text{latt}}(\text{MF}_3)$ and $E_{\text{latt}}(\text{AlF}_3)$ are the lattice energies of the rare-earth fluoride MF₃ and of AlF₃ respectively, and $E_{\text{subs}}(\text{Al}^{3+})$ is the energy of substitution at the Al³⁺ site.

3. Results

3.1. Perfect lattice properties

The potentials derived are given in table 1. Calculated perfect lattice properties are reported for both forms of topaz in table 2. It is seen that the potential derived for both forms of topaz reproduces the lattice parameters with an accuracy of approximately $\pm 1\%$, and it is noted that atomic positions are also reproduced to within $\pm 2\%$, which is consistent with the performance of potentials for related complex materials. For OH⁻-topaz it is noted that there are two distinct H positions for each OH⁻ group. The simulated (experimental) structure has equal occupancy of both sites, but it is noted from table 3 that a structure based on full occupancy of either site has higher stability.

Table 2. Calculated and experimental perfect lattice parameters for topaz.

Lattice parameter	Experimental [1]	Calculated	Difference (%)
$\text{Al}_2\text{SiO}_4\text{F}_2$			
a (Å)	4.652	4.694	0.91
b (Å)	8.801	8.746	-0.62
c (Å)	8.404	8.491	1.04
$\text{Al}_2\text{SiO}_4(\text{OH})_2$			
a (Å)	4.720	4.686	-0.71
b (Å)	8.920	8.934	0.16
c (Å)	8.418	8.505	1.02

Table 3. Calculated lattice energies for F^- - and OH^- -topaz.

Topaz form	Lattice energy (eV)
$\text{Al}_2\text{SiO}_4\text{F}_2$	-275.39
$\text{Al}_2\text{SiO}_4(\text{OH})_2$ (50:50 H1:H2)	-297.26
$\text{Al}_2\text{SiO}_4(\text{OH})_2$ (100% H1)	-298.37
$\text{Al}_2\text{SiO}_4(\text{OH})_2$ (100% H2)	-298.38

Table 4 compares calculated and measured IR and Raman frequencies, which represent an additional test for the potential. Calculated phonon frequencies are listed in the first two columns, for F^- - and OH^- -topaz respectively. The third column lists the experimental infrared (IR) or Raman (R) peak positions measured by a number of authors (listed in the fourth column). The vibration mode assignments (fifth column) were based on the work of a number of previous authors [12–14]. It is seen that very good agreement is obtained for most frequencies, showing that the potential describes both topaz species reliably. Some interesting conclusions can be drawn.

- (i) The calculations confirmed the proposed assignment [12] that the 314 and 325 cm^{-1} modes are related to Al–F groups, since in the simulations frequencies in this region were obtained only for F^- -topaz and not for OH^- -topaz.
- (ii) Similarly, the 1060 cm^{-1} mode attributed to Al–OH modes [12, 13] could only be seen in the OH^- -topaz simulations, confirming this assignment.
- (iii) The simulations support the assignment of the 1160–1188 cm^{-1} modes to either Al–OH [3] or in-plane bending O–H modes [12], since no frequencies in this range were obtained in the F^- -topaz simulations.
- (iv) The 1079, 1080 cm^{-1} modes are likely to be due to interstitial OH^- groups [12, 13], rather than to Al–OH modes [16], since they are not detected in the calculations, which model non-defective topaz.
- (v) It is suggested that the 738, 732 and 775 cm^{-1} modes, not yet assigned, are related to OH^- -containing groups, since they were only observed in the simulations of OH^- -topaz, while the modes between 236–268, 370–457 and 619–655 cm^{-1} are likely to be related to groups that do not contain either F^- or OH^- species, since they were found with similar calculated values in both topaz species.
- (vi) The 3290–3330, 3423 and 3486 cm^{-1} modes could be due to OH^- groups, as proposed [16, 2]. However, these modes do not appear in the OH^- -topaz simulations, and are therefore more likely to come from interstitial OH^- groups.

Table 4. Experimental and calculated IR and Raman frequencies.

F ⁻ -topaz	OH ⁻ -topaz	Exp. values	References	Assignment [13, 14]
	235			
236	236	236–241	[12–14]	
241	243			
268	269	265–268	[12, 13]	
	285			
283	286	284–288	[12–14]	ν_2 (R) sym. def. SiO ₄
	287			
	289			
	298			
299	301	300–320	[12, 13]	Al–O
303	306			
312	311			
315		314	[12]	Al–F
324		325	[12]	Al–F
	374			
370	377	370–380	[12, 13]	
379	378			
	379			
	381			
	401			
397	401	400–425	[12, 13, 16, 17]	
405	416			
413	417			
418	423			
4512	450			
453	452	445–457	[12, 13, 16, 17]	
454	452			
456	456			
484	490	483–494	[13, 14, 16, 17]	ν_1 (IR) sym. stretch SiO ₄
485	493			
487				
	519			
524	528	518–530	[12–14]	ν_1 (IR) sym. stretch SiO ₄
	529			
	530			
542	540	541–548	[12, 13]	ν_1 (IR) sym. stretch SiO ₄
545				
557	555	559–562	[12–14, 16, 17]	ν_4 (R) antisym. bend SiO ₄
	556			
619	633			
627	634	619–635	[16, 17]	
633	635			
638	645	640–655	[2, 3, 7]	
	712			
	714			
	717	708, 732	[16, 17]	
	723			
	726			

Table 4. (Continued.)

F ⁻ -topaz	OH ⁻ -topaz	Exp. values	References	Assignment [13, 14]
	772			
	773	775	[17]	
	775			
840	845	842–845	[12–14, 16]	ν_3 (R) antisym. stretch
842				
890	882	880–935	[12–14, 17]	ν_1 (R) sym. stretch. SiO ₄
904	899			
938				
	956			
961	970	950–985	[12, 13, 17]	ν_3 (R) SiO ₄
	977			
	986			
	1018	1005–1010	[12, 13, 17]	ν_3 (R) SiO ₄
	1048	1060	[12, 13, 17]	Al–OH
			[12, 13, 17]	ν_{bending} O–H
		1079, 1080	[16]	or Al–OH
	1179			
	1180	1160–1188	[13, 16, 17]	$\nu_{\text{in-plane bending}}$ O–H
	1181			or
	1186		[12]	Al–OH
		3290–3330	[16, 17]	ν_{stretch} O–H
		3423	[2]	ν_{stretch} O–H
		3486	[2]	ν_{stretch} O–H
	3558			
	3559	3520, 3585	[13, 15, 16, 2]	ν_{stretch} O–H
	3564			
	3565			
		3625 (IR)		
	3641.85	3639 (R)	[13, 2, 18]	ν_{stretch} O–H
	3642.22	3647 (IR)		
		3650 (IR)		
	3800			
	3804	3850	[17]	ν_{stretch} O–H
	3805			
	3811			

3.2. Point defects in topaz

Table 5 gives defect formation energies for basic intrinsic defects in both forms of topaz. These can be made more meaningful by calculation of the corresponding Frenkel and Schottky energies, which are reported in table 6. From this table it can be seen that for F⁻-topaz, fluoride Frenkel or Schottky disorder is the lowest energy process, and also that exchange between Al and Si, and between O and F, may occur. However, for OH⁻-topaz it is striking that the lowest energy process is OH⁻ Frenkel formation, which, as noted in the previous section, is confirmed by the existence of infrared frequencies corresponding to free OH⁻ groups in the structure.

Table 5. Calculated basic intrinsic defect formation energies.

Defect species	Formation energy in Al ₂ SiO ₄ F ₂ (eV)	Formation energy in Al ₂ SiO ₄ (OH) ₂ (50:50) (eV)
V _{Si}	100.91	117.06
V _{Al}	56.48	83.82
V _{O1}	23.70	25.10
V _{O2}	24.41	25.10
V _{O3}	23.39	25.51
V _F	3.91	—
V _{OH}	—	16.07
Si _i	-78.20	nc ^a
Al _i	-43.92	-42.67
O _i	-14.83	-13.67
F _i	1.51	—
OH1 _i	—	-14.01
OH2 _i	—	-14.09
Al _{Si}	39.79	39.11
Si _{Al}	-37.40	-36.17
O _F	-15.46	—
F _{O1}	18.17	—
F _{O2}	18.49	—
F _{O3}	18.57	—
O _{OH}	—	-4.69

^a 'nc' means that the calculation did not converge.

Table 6. Calculated Frenkel, Schottky and ion exchange energies.

Defect species	Formation energy in Al ₂ SiO ₄ F ₂ (eV)	Formation energy in Al ₂ SiO ₄ (OH) ₂ (50:50) (eV)
Si Frenkel	22.71	nc
Al Frenkel	12.56	41.15
O1 Frenkel	8.87	11.43
O2 Frenkel	9.58	11.43
O3 Frenkel	8.56	11.84
F Frenkel	5.42	—
OH1 Frenkel	—	2.06
OH2 Frenkel	—	1.98
Schottky (per defect)	4.58	13.42
Al-Si exchange	2.39	2.94
O1-F exchange	2.71	—
O2-F exchange	3.03	—
O3-F exchange	3.11	—

Al and Si antisites may also occur, as observed in the case of F⁻-topaz. This result is supported by the observation of luminescence spectra due to (AlO₄)⁰ [19–21], a centre formed when Al substitutes at the Si site and an extra hole is captured to neutralize the defect.

Table 7. Substitution energies (E_{sub}) and solution energies (E_{sol}) for dopants at Al^{3+} and Si^{4+} sites in topaz.

Dopant	$E_{\text{sub}}(\text{Al}^{3+})$	$E_{\text{sub}}(\text{Si}^{4+})$	$E_{\text{sol}}(\text{Al}^{3+})$	$E_{\text{sol}}(\text{Si}^{4+})$
F^- -topaz				
Ti^{3+}	5.19	44.37	2.12	2.64
Cr^{3+}	-6.02	34.97	-2.27	0.06
Mn^{3+}	4.08	43.93	3.75	4.94
Fe^{3+}	0.52	44.17	3.77	8.76
OH^- -topaz				
Ti^{3+}	6.02	43.79	1.15	2.86
Cr^{3+}	-4.93	34.21	1.62	4.7
Mn^{3+}	5.84	43.44	1.33	2.87
Fe^{3+}	6.31	43.78	1.15	2.37

3.3. Dopant substitution and solution energies

Table 7 reports solution energies for Ti^{3+} , Cr^{3+} , Mn^{3+} , and Fe^{3+} . From these energies, it is clear that substitution at the Al^{3+} site is energetically preferred, although there are some interesting observations that can be made.

- (i) Cr^{3+} has a low solution energy at the Si^{4+} site in F^- -topaz, making substitution at this site a possibility, although substitution at the Al^{3+} site is still preferred.
- (ii) Ti^{3+} , Mn^{3+} and Fe^{3+} show an energetic preference for substitution in OH^- -topaz rather than in F^- -topaz.

4. Discussion and conclusions

The paper has described the derivation of a potential for the calculation of the perfect lattice and defect properties of F^- and OH^- -topaz. As well as showing good agreement between experimental and calculated frequencies, the calculations enable the measured frequencies to be assigned, and suggest that two infrared frequencies correspond to free OH^- groups. Defect calculations predict the existence of these OH^- groups by suggesting that OH^- interstitial formation will be favoured. For F^- -topaz, Schottky defect formation is slightly favoured over F^- Frenkel formation. Regarding ion implantation, Cr^{3+} is the only ion predicted to be easier to implant in F^- -topaz than in OH^- -topaz, and in all cases of the ions considered, substitution at the Al^{3+} site is energetically favoured. For device manufacture where implantation is part of the process, OH^- -topaz is therefore likely to be a better starting material.

Acknowledgments

The authors thank the CNPq and CAPES for financial support.

References

- [1] Northrup P A, Leinenweber K and Parise J B 1994 *Am. Mineral.* **79** 401
- [2] Souza D N, Lima J F, Valerio M E G, Fantini F, Pimenta M A, Moreira R L and Caldas L V E 2002 *Nucl. Instrum. Methods B* **191** 230

- [3] Wondraczek L, Heide G, Kilo M, Nedeljkovic N, Borchardt G and Jackson R A 2002 *Phys. Chem. Minerals* **29** 341
- [4] Jackson R A and Catlow C R A 1988 *Mol. Simul.* **1** 207
- [5] Marques C, Falcão A, da Silva R C and Alves E 2000 *Nucl. Instrum. Methods B* **166/167** 204
- [6] Souza D N, Lima J F, Valerio M E G, Alves E and Caldas L V E 2002 *Nucl. Instrum. Methods B* **191** 196
- [7] Gale J D 1997 *J. Chem. Soc. Faraday Trans.* **93** 629
- [8] Grau-Crespo R, Peralta A G, Ruiz-Salvador A R, Gomez A and Lopez-Cordero R 2000 *Phys. Chem. Chem. Phys.* **2** 5716
- [9] Mott N F and Littleton M J 1938 *Trans. Faraday Soc.* **34** 485
- [10] Catlow C R A 1989 *J. Chem. Soc. Faraday Trans. 2* **85** 335
- [11] Amaral J B, Plant D F, Valerio M E G and Jackson R A 2003 *J. Phys.: Condens. Matter* **15** 2523
- [12] Kloprogge J T and Frost R L 2000 *Spectrochim. Acta A* **56** 501
- [13] Beny J M and Piriou B 1987 *Phys. Chem. Minerals* **15** 148
- [14] Griffith W P 1969 *J. Chem. Soc. A* (9) 1372
- [15] Wunder B, Rubie D C, Ross C R II, Medenbach O, Seifert F and Schreyer W 1993 *Am. Mineral.* **78** 285
- [16] Wunder B and Marler B 1997 *Eur. J. Mineral.* **9** 1147
- [17] Gadsden J A 1975 *Infrared Spectra of Minerals and Related Compounds* (London: Butterworth)
- [18] Pinheiro M V B, Fantini C, Krambrock K, Persiano A I C, Dantas M S S and Pimenta M A 2002 *Phys. Rev. B* **65** 104301
- [19] Souza D N, Valerio M E G, Lima J F and Caldas L V E 2000 *Nucl. Instrum. Methods B* **166/167** 209
- [20] Souza D N, Valerio M E G, Lima J F and Caldas L V E 2002 *Radiat. Prot. Dosim.* **100** 413
- [21] Souza D N, Valerio M E G, Lima J F and Caldas L V E 2003 *Appl. Radiat. Isot.* **58** 489